Proc. Natl. Acad. Sci. USA
Vol. 95, pp. 2801–2806, March 1998
Biochemistry

The crystal structure of *Pyrococcus furiosus* ornithine carbamoyltransferase reveals a key role for oligomerization in enzyme stability at extremely high temperatures

VINCENT VILLERET*, BERNARD CLANTIN†, CATHERINE TRICOT‡, CHRISTIANNE LEGRAIN‡, MARTINE ROOVERS§¶, VICTOR STALON†, NICOLAS GLANSDORFF‡§¶, AND JOZEF VAN BEEUMEN*‖

*Laboratorium voor Eiwitbiochemie en Eiwitengineering, Universiteit Gent, Ledeganckstraat 35, B-9000 Gent, Belgium; and †Laboratoire de Microbiologie, Université Libre de Bruxelles, ‡Institut de Recherches du Centre d'Enseignement et de Recherches des Industries Alimentaires, Commission de la Communauté Française de Belgique, Région Bruxelles Capitale, §Laboratorium voor Erfelijkheidsleer en Microbiologie, Vrije Universiteit Brussel, and ¶Vlaams Interuniversitair Instituut voor Biotechnologie, avenue E. Gryson 1, B-1070 Brussels, Belgium

Edited by Max F. Perutz, Medical Research Council, Cambridge, United Kingdom, and approved January 5, 1998 (received for review September 8, 1997)

ABSTRACT **The *Pyrococcus furiosus* (PF) ornithine carbamoyltransferase (OTCase; EC 2.1.3.3) is an extremely heat-stable enzyme that maintains about 50% of its activity after heat treatment for 60 min at 100°C. To understand the molecular basis of thermostability of this enzyme, we have determined its three-dimensional structure at a resolution of 2.7 Å and compared it with the previously reported structures of OTCases isolated from mesophilic bacteria. Most OTCases investigated up to now are homotrimeric and devoid of allosteric properties. A striking exception is the catabolic OTCase from *Pseudomonas aeruginosa*, which is allosterically regulated and built up of four trimers disposed in a tetrahedral manner, an architecture that actually underlies the allostery of the enzyme. We now report that the thermostable PF OTCase (420 kDa) presents the same 23-point group symmetry. The enzyme displays Michaelis–Menten kinetics. A detailed comparison of the two enzymes suggests that, in OTCases, not only allostery but also thermophily was achieved through oligomerization of a trimer as a common catalytic motif. Thermal stabilization of the PF OTCase dodecamer is mainly the result of hydrophobic interfaces between trimers, at positions where allosteric binding sites have been identified in the allosteric enzyme. The present crystallographic analysis of PF OTCase provides a structural illustration that oligomerization can play a major role in extreme thermal stabilization.**

On the basis of 16S tRNA sequence data, the Archaea appear to represent a phylogenetically distinct evolutionary domain whose members possess various extraordinary properties, including the ability of some species to grow at temperatures of about 100°C (1, 2). The proteins from these organisms usually display extreme thermostability and the analysis of their structures is expected to provide insights into the underlying molecular mechanisms.

The biosynthesis of arginine has been extensively investigated in a broad variety of organisms (3–5), but data concerning thermophilic prokaryotes became forthcoming only recently (5–8). The sixth step of the arginine biosynthetic pathway is catalyzed by ornithine carbamoyltransferase (OTCase), which produces citrulline from ornithine and carbamoylphosphate (CP) and usually displays Michaelis–Menten kinetics. CP also is required for pyrimidine biosynthesis. The half-life of this highly thermolabile precursor at neutral pH in aqueous solution is less than 1 sec at 100°C; moreover, CP decomposition produces cyanate, an indiscriminate carbamoylating agent (8). The involvement of such a thermolabile intermediate in the metabolism of extreme thermophilic microorganisms raises the question of which mechanisms protect it from decomposition at elevated growth temperatures. Recent results suggest that in *Thermus aquaticus* and *Pyrococcus furiosus* (PF), CP is protected from the bulk of the aqueous phase by channeling between carbamoylphosphate synthetase and OTCase (8, 9). The molecular analysis of the protein–protein interactions assembling the cognate enzymatic complex requires a detailed structural study of the partner proteins.

Besides anabolic OTCases involved in the arginine biosynthetic pathway, a catabolic OTCase converting citrulline into ornithine and carbamoylphosphate is found when the arginine deiminase pathway is present, such as in *Pseudomonas aeruginosa* (PA) where the enzyme has been investigated in much detail (10–12). This catabolic OTCase displays marked cooperativity toward CP and is allosterically activated by nucleoside monophosphates or inorganic phosphate, and inhibited by polyamines such as spermidine or putrescine. These allosteric properties are essential as they allow the enzyme to function in the catabolic direction of the reaction catalyzed by OTCase. So far 33 OTCase sequences have been reported, of which the one from PF is the only archaeabacterial enzyme, but only two crystal structures, that from a mutant form of PA catabolic OTCase (13) and that from the anabolic OTCase from *Escherichia coli* (14), have been reported. Despite high sequence identities between these enzymes, large differences at the level of the quaternary structures are observed. Catabolic OTCase is a protein of 456 kDa composed of four trimers disposed in a tetrahedral manner, following the 23-point group symmetry (13, 15). The allosteric properties of catabolic OTCase can be correlated to its highly symmetrical oligomeric structure, because the modification of residues located at trimer interfaces leads to the production of trimeric and active Michaelian enzymes (12). On the other hand, the *E. coli* anabolic OTCase, as well as all other anabolic OTCases investigated up to now, are trimers of about 105 kDa also displaying Michaelis–Menten kinetics.

As part of a study of carbamoylphosphate metabolism in thermophilic microorganisms, we recently isolated and characterized from PF an OTCase that is active at very high temperatures. The purified OTCase displays thermostability,

The publication costs of this article were defrayed in part by page charge payment. This article must therefore be hereby marked "*advertisement*" in accordance with 18 U.S.C. §1734 solely to indicate this fact.

This paper was submitted directly (Track II) to the *Proceedings* office.

Abbreviations: OTCase, ornithine carbamoyltransferase; CP, carbamoylphosphate; PF, *Pyrococcus furiosus*; PA, *Pseudomonas aeruginosa*.

Data deposition: The structure reported in this paper has been deposited in the Protein Data Bank, Biology Department, Brookhaven National Laboratory, Upton, NY 11973 (reference no. 1a1s).

‖To whom reprint requests should be addressed. e-mail: jozef.vanbeeumen@rug.ac.be.

with half-lives of 40–65 min at 100°C; it does not exhibit allosteric properties (16). The molecular mass of the enzyme is very high (>400 kDa) suggesting that *Pyrococcus* OTCase probably adopts a quaternary structure similar to that of the allosteric homologue from *Pseudomonas* (16). To elucidate the role of this quaternary organization in enzyme stability we have determined the crystal structure of the thermophilic OTCase.

Protein Isolation and Crystallization. The PF OTCase has been overexpressed in *Saccharomyces cerevisiae* (17) and purified following the protocol described in Marcq *et al.* (15) but with a thermal denaturation for 10 min at 75°C added as the first purification step. The overexpressed OTCase has the same catalytic properties and the same behavior at high temperatures as the native enzyme (16). From the electron density map we identified that S171 has an extra density, which, from the difference of the sequence-based molecular mass (35,050 Da) with the effective value measured by electrospray mass spectrometry (35,080 Da, B. Devreese, personal communication) could not be assigned. The crystals of OTCase were grown by vapor diffusion by using the hanging-drop method. They formed at 21°C in 10-μl droplets of a 1/1 volume mixture of 12 mg·ml^{-1} of protein solution and a reservoir solution containing 1 M NaCl in 100 mM acetate buffer (pH 4.0). Crystals of a typical size of 0.5 mm^3 where obtained after 7–10 days.

Data Collection. Data were collected with a MacScience DIP2030 image plate system, using the CuKα radiation produced by a Nonius FR591 rotating anode generator equipped with a double mirror x-ray optical system and running at 100 mA, 45 kV. The space group is F23 with unit cell parameters a=b=c=186.8 Å. There is one monomer in the asymmetric unit and four dodecamers in the unit cell. A data set has been measured to 2.7 Å resolution. The data are 99.3% complete from 30.0 to 2.7 Å resolution and the R_{merge} on intensities is 6.4% based on 184,193 measured observations. These data, processed by using the program DENZO (18), have been reduced to 14,853 unique reflections between 30.0 Å to 2.7 Å resolution.

Structure Determination and Refinement. The structure was determined by using the molecular replacement method with the AMORE program (19). Initial trials were conducted in space group F23 by using one polyalanine monomer of the allosteric catabolic OTCase as a model. No clear rotation solution emerged, and testing a very large number of rotation solutions in the translation function did not lead to the correct solution. The diffraction data were reprocessed in space group F222 where there is one trimer per asymmetric unit. Molecular replacement using one polyalanine trimer as a search model led to a solution in this space group displaying a correlation coefficient of 0.31 and a *R* factor of 0.50 after rotation and translation searches, and rigid-body refinement. Subsequent rigid body refinements were carried out by using X-PLOR (20), through which the two domains of each monomer were refined as single rigid-body units. A dramatic increase of the correlation coefficient to 0.48 and a decrease of the *R* factor to 0.47 were observed, resulting from a 8° rotation of the ornithine binding domain relative to the carbamoylphosphate binding domain. This modified monomer subsequently was used as a search model for the molecular replacement in the correct space group F23. It resulted in a similar solution to the one found in space group F222.

Side chains were included, and the model was refined with the X-PLOR slow cooling protocol followed by energy minimization. The R_{free}, using 10% of data, was monitored throughout the refinement and displayed a final value of 0.254. The final *R* factor is 0.213 against all working set data from 10.0–2.7 Å, without solvent molecules added. The loop comprising residues 235–245 and also the two C-terminal residues show very weak electron densities, explaining in part why a lower final *R* factor is not observed. The model has an acceptable stereochemistry with rms values of bond length and bond angle of 0.009 Å and 1.7°, respectively.

Overview of the Dodecamer. The thermophilic OTCase crystallizes in space group F23, with one monomer per asymmetric unit. Thus the enzyme is a dodecamer of exact 23-point group symmetry. The basic catalytic structural motif in carbamoyltransferases such as OTCases and aspartate carbamoyltransferases is a homotrimer with one active site per monomer (21). The trimers, referred to as "catalytic trimers," have convex faces. The thermophilic oligomer is composed of four catalytic trimers disposed in a tetrahedral manner, with the convex faces of the trimers pointing toward the inner side of the particle (Fig. 1*A*). When looking at the structure as a tetrahedron, the four 3-fold symmetry axes pass through the middle of the faces, and the three 2-fold symmetry axes pass through the middle of opposite edges. The diameter of the structure is 130–135 Å when viewed along a 3-fold or a 2-fold symmetry axis and an internal cavity is present at the center of the particle, with an approximate diameter of 25–30 Å.

Description of the Structure. The monomer comprises 314 amino acid residues and folds into two domains of similar size. The N- and C-terminal domains are referred to as the CP binding and ornithine binding domains, according to their respective involvements in substrate recognition. Each domain is organized around a β pleated sheet of five parallel strands surrounded by α helices. Helices H5 and H12 link the two domains, with H12 passing through the two domains (Fig. 1*B*). The active site is located in a pocket between the domains; it is delimited by helices H2, H12, and H5 and the sequence segment containing the residues HCLP located between strand B10 and helix H11 (residues 268–271). As in PA OTCase, charged interactions appear to stabilize the relative positions of helices H1, H5, and H12, which constitute an important structural motif on which the dodecamer is built (Table 1). Residues K31, E147, and E295, three residues involved in these interactions, are present in all OTCases sequenced so far, and thus are expected to be essential for the structural integrity of the OTCase monomer. Also observed between H1 and H5 is an aromatic interaction involving W21 (H1) and W146 (H5), with their side chains disposed in a perpendicular way at a distance of 4 Å. However the NH group of one Trp indole does not point at the π electrons of the neighboring indole ring of the other Trp residue. Aromatic interactions also occur between F30, W33, and H40 and may stabilize the position of W33, a crucial residue in trimer–trimer interfaces within the dodecamer (see below). The N-terminal region is well-defined in the electron density map and appears stabilized through interactions of the amino terminal group with the side chain of E18 and also with residues from other monomers in the dodecameric assembly (described below). A salt bridge between R7 and E19 could stabilize the N-terminal residues that form a closed loop around helix H1.

The interfaces between the monomers within the catalytic trimers involve mainly the three CP binding domains (Fig. 1*C*). Helix H3 from one monomer is positioned in front of helix H12 of the second monomer, with the loop comprising residues 78–83 located near the catalytic site of the adjacent monomer. A characteristic feature of this interface is the presence of ion pair networks (Table 2): one network involves residues D284-R274 of monomer 1 and residues D92-R95 of monomer 2, the second network involves E295-K35-D292 (monomer 1) and R99 (monomer 2), and the last one comprises E44-R41 (monomer 1) and R41-E44 (monomer 2). The second network is composed of residues mentioned above as being important also for the stabilization of helices H1 and H12 within the monomer.

The main interfaces that occur between trimers in the dodecameric assembly are located around the 3-fold symmetry axes, at the four tops of the tetrahedral oligomer. Helices H1 from three monomers (belonging to different catalytic trimers

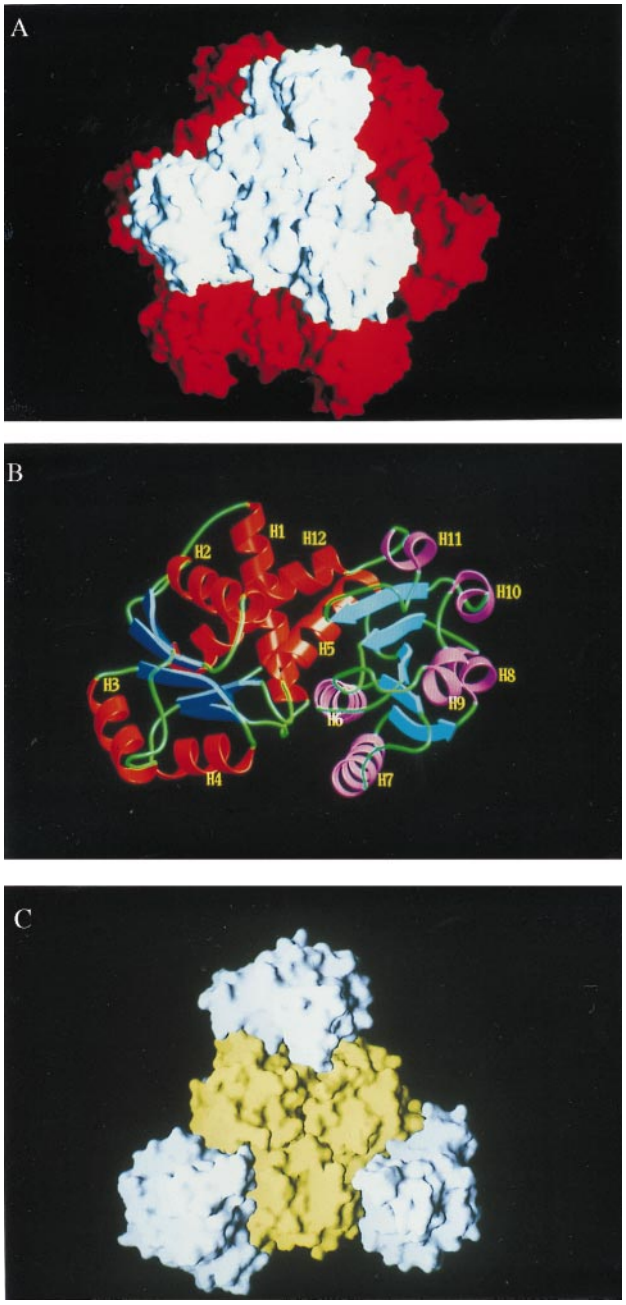

FIG. 1. (*A*) Molecular surface illustration of the dodecameric oligomer, where one trimer is represented in white and the three other trimers in red. The molecule has an approximate diameter of 130 Å. (*B*) Ribbons drawing of the OTCase monomer. Helices from the CP binding domain and H12 are in red; helices from the ornithine binding domain are in pink. Each domain is organized around a β pleated sheet of five parallel strands, respectively, from top to bottom: B3, B2, B4, B5, and B1 for the CP binding domain (deep blue) and B10, B9, B6, B7, and B8 for the ornithine binding domain (light blue). (*C*) Molecular surface illustration of a trimer viewed along its 3-fold symmetry axis. The three CP binding domains are in yellow and the ornithine binding domains in white. Figures were generated by using GRASP (35) (*A* and *C*) and MOLSCRIPT (36) and RASTER3D (37) (*B*).

and referred to as "structural trimers") are facing each other around the symmetry axis and constitute a hydrophobic interface involving M29, I32, W33, and I36 of each helix H1 (Fig. 2*A*). K38 also is located in this interface and is exposed to solvent, but in the internal cavity of the molecule. This lysine interacts with the CO group of P39 from the same catalytic chain. These residues form "rings" around the 3-fold symmetry axis composed of three tryptophans, six isoleucines, three methionines, and three lysines. The hydrophobic stem of the side chain of K38 also contributes to the hydrophobic interface. When moving away from the symmetry axis, interactions involving residues that belong to H5 or H1 of one monomer and the N-terminal residue of a second monomer are observed: between the side chain of E147 and the amino group of V1, and between the side chain of K31 and the carbonyl group of V1. A salt bridge is also present between K28 and E25 of each pair of monomers, thus resulting in three salt bridges around each 3-fold symmetry axis (Fig. 2*A*).

Table 1. Main interactions observed between helices H1, H2, H5, and H12 within the monomers

PF OTCase	PA OTCase
K31(H1)-E147(H5)	K31(H1)-E315(H12)
	K31(H1)-E147(H5)
K35(H1)-E295(H12)	E39(H1-B2)-K325(H12)
K148(H5)-D292(H12)	H148(H5)-E315(H12)

Each monomer also is involved in an interface located around a 2-fold symmetry axis. C-terminal residues of two monomers that belong to different catalytic trimers are facing each other and cover a 15 Å channel penetrating into the structure and joining the internal cavity previously mentioned. No specific interactions are identified at this interface, suggesting a minor role in the dodecameric assembly.

Structural Comparison of Allosteric and Thermophilic OTCases. The quaternary structures of PA and PF OTCases differ in many aspects, from domain movements within the subunits to rotations of trimers around their 3-fold symmetry axes. This results in large differences in subunit interfaces that can be related to allostery or thermophily in the respective OTCases.

The monomer of PA OTCase contains 335 residues (314 residues in PF OTCase) and displays the same overall topology as PF OTCase; there is 39% sequence identity between the two enzymes (16). The difference in length between the two sequences is largely explained by the presence of an additional α helix in PA OTCase (helix H10′). However, the role of this secondary structure element is not a crucial one because it is fully exposed to the solvent and does not take part in the formation of the quaternary structure. Moreover, based on the sequence alignments, this secondary structure element is not specific to catabolic enzymes because a similar α helix also is found in some anabolic OTCases, for example in *E. coli* and *Neisseria gonorrhoeae*. Besides the absence of helix H10′, four deletions of one residue are observed in PF OTCase, namely in the loops H5-B6, B6-H6, B9-H9, and H10-B10. There are also two insertions at the C terminus in PF OTCase.

The main difference between the monomers of PF and PA OTCases can be seen when the two CP domains are superimposed. There is a 8° difference in the orientation of the ornithine binding domains resulting in domain closure in PF OTCase (Fig. 3). This rotation takes place at two hinge regions located at the end of helix H5 (residues 148–149) and just before the beginning of helix H12 (residue 286–287). Thus, H12 behaves as a part of the CP domain with a conserved orientation in the two OTCases. The rms deviation calculated on Cα is 1.3 Å for the CP domains and 1.7 Å for the ornithine binding domains, reflecting the rotation as a rigid body of a well-conserved structural motif. The N-terminal residues have different conformations and form a closed loop in PF OTCase whereas they display an open conformation in PA OTCase. As in PF OTCase, interactions stabilizing the orientation of H1, H5, and H12 relative to the CP domain also are found in PA OTCase (Table 1). Most of these interactions are identical or structurally located at equivalent positions to those observed in PF OTCase and probably are required to preserve the structural integrity of OTCase monomers.

Table 2. Main interactions observed between two monomers within the catalytic trimers

PF OTCase		PA OTCase	
Monomer 1	Monomer 2	Monomer 1	Monomer 2
D284-R274(H11-H12)	D92-R95 (H3)	E307(H11-H12)	D92-R95-K91 (H3)
K35(H1)-E295(H12)-K148(H5)-D292(H12)-	R99 (H3) R99(H3)	E318 (H12)	R99 (H3)
E44-R41 (H11-H12)	R41-E44 (H1-B2)	R58 (H2)	E88 (B3-H3)

The catalytic trimers of PF and PA OTCase show a conserved organization, an observation that could have been anticipated because the formation of the active site results from the association of individual polypeptides into a trimer. However, a small reorientation of 1.8° is observed when comparing the relative orientations of the CP domains within the trimers. As in PF OTCase, this interface involves the positioning of helix H3 in front of helix H12 of another monomer and is stabilized via charged interactions: E318 (H12)-R99 (H3), R58 (H2)-E88 (B3-H3). There also occur ion pair networks composed of D92, R95, K91 (monomer1), and E307 (monomer 2) (Table 2). The interaction involving R58 and E88 is not observed in PF OTCase, although the two residues are present. This interaction occurs close to the binding site of the phosphate group of CP, and it is expected, by analogy to observations made for the paralogous enzyme aspartate carbamoyltransferase (21), that the loop comprising residue 88 undergoes a conformational change when substrate binding occurs.

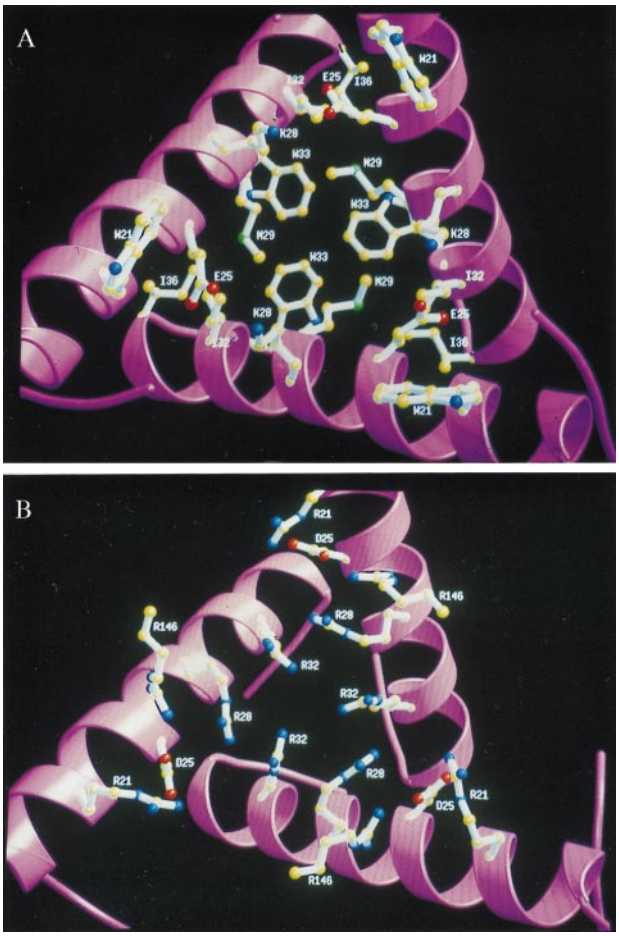

FIG. 2. View of the interface between trimers located around a 3-fold symmetry axis at one top of the dodecamer. The three H1 helices from CP domains that belong to three monomers are shown in ribbons. (*A*) Interface in PF, mainly composed of the hydrophobic residues W21, M29, I32, W33, and I36. The salt bridges between K28 and E25 also are shown. (*B*) Interface in PA composed of positively charged residues: R21, R28, R32, and R146, constituting a binding site for negatively charged allosteric effectors. The difference in compactness between both enzymes also is illustrated by the increased packing in the PA OTCase of the three helices H1 around the 3-fold symmetry axis. Figures were generated by using MOLSCRIPT (36) and RASTER3D (37).

Large differences are observed between the quaternary structures of the two dodecamers. Rotations of the catalytic trimers of 6° around their respective 3-fold symmetry axes occur in opposite directions, resulting in drastically altered interfaces. At the top of the tetrahedral oligomer in PA OTCase, helices H1 still constitute the interface between three monomers from different catalytic trimers, but they are partially covered, because of the rotation of the ornithine domain, by the loop H5-B6 located just after the hinge region identified within the monomer (residues 150–155). Helices H1 do not show the strong hydrophobic character observed in PF OTCase; instead they comprise three arginines (in positions 21, 28, and 32), which point toward a sulfate or phosphate ion identified in the x-ray structure as being located on the 3-fold symmetry axis (13). One arginine from helix H5 (R146) is also present in this interface, forming, along with residues 32, 28, and 21, rings of positively charged residues around the 3-fold symmetry axis (Fig. 2*B*). R32 is in close contact with the oxygen of the ion (2.8 Å), as is R28 (3.8 Å). The rings formed by R146 and R21 are located further from the ion and do not interact directly. Within the PA OTCase monomer, two aspartate residues, D25 and D29 in helix H1 are in close contact with R21, R28, and R32. D25 is located between R21 and R28, and D29 is located between R28 and R32. They may contribute to stabilizing the relative positions of all of these positively charged residues, creating an interface specially designed to bind negatively charged compounds. The three loops H5-B6, and more specifically residues 150–153 (located after the hinge residues of helix H5), partially cover the arginine rings (not shown). A proline in position 152 may stabilize the loop conformation, just at the beginning of the ornithine binding domain. These domains are also in close contact in the dodecamer through residues P266-R267 (loop H10-B10) from one monomer and residues E147-D154 (loop H5-B6) and E207 (helix H7) from another monomer. Such contacts are not found in PF OTCase because of the domain closure observed within the monomer, resulting in a significant increase of the distance between the ornithine binding domains of different monomers in the dodecameric assembly.

The contacts between monomers from different catalytic trimers around the 2-fold symmetry axes are more extended in PA OTCase because of the higher compactness of the overall structure. As mentioned earlier, the N-terminal residues have a more open conformation and interact with residues from the sequence segment G98-G122 (between helices H3 and H4). Amino groups of the side chain of R45 (loop H1-B2) interact with the main-chain carbonyl groups of the C-terminal residues, D334 and I335. Six interfaces of this type are present in the dodecamer. No apparent channel is observed in PA OTCase, resulting from the compactness of the structure, although an internal cavity is also present in the catabolic enzyme. This interface between monomers from different catalytic trimers is expected to play a role in the allosteric behavior of the protein: mutants where the C-terminal residues have been deleted show altered response toward allosteric

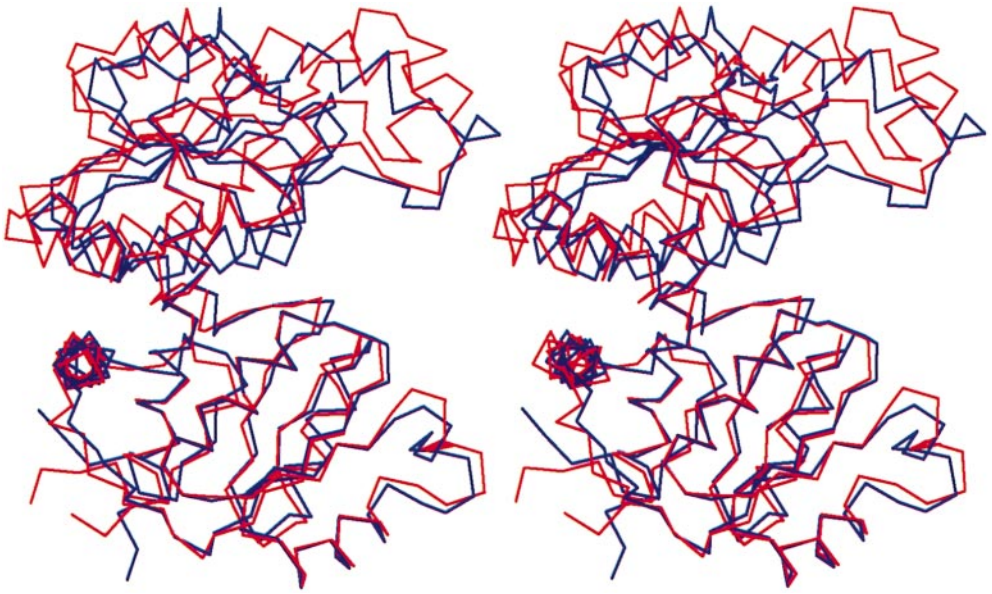

FIG. 3. Stereo view of the Cα backbone of PF (blue) and PA (red) monomers, where the two CP binding domains have been superimposed. The ornithine binding domains differ in a rotation of 8°, resulting in a domain closure in PF OTCase. The CP binding domains are at the bottom. The figure was generated by using MOLSCRIPT (36).

inhibitors (11). However the exact role in effector binding and/or signal transmission of this interface needs to be further investigated.

Functional Implications. Recent structural analyses of proteins from extreme thermophilic and hyperthermophilic organisms provide closer insight into the different strategies that nature developed for stabilizing the native conformation of proteins at extreme temperatures. Several features have been discussed, such as the ratio of the different residue types (22), an increase of the number of ion bridges and/or of hydrophobic interactions (23–27), the reduction of solvent accessible area resulting from an increased compactness of the structures (27–29), the stabilization of α-helices, strengthening of N- and C-terminal regions of the polypeptide chain (30), or the shortening of loops (31).

Comparative examination of the primary structures of OTCases did not point to any obvious features that could explain the high thermostability of PF OTCase, except a reduction in asparagine residues (known to be thermolabile if exposed to the solvent) and an increase of tryptophan residues (known to make more hydrophobic interactions). However, from the three-dimensional structure of PF OTCase, the decrease in asparagine content does not appear to play a crucial role in the protein stability, even though the three asparagines found in PA OTCase (residues 3, 6, and 8) at the N terminus are replaced by Ser, Gly, and Asp, respectively. It is not currently known whether the substitution of these asparagines is of significance regarding the conformational stability of N-terminal residues involved in trimer–trimer interfaces.

The increased proportion of tryptophan residues in PF OTCase does appear, on the other hand, to be a significant feature. Two tryptophans in position 21 and 33 are found in helix H1 where they structurally occupy the positions of arginine 21 and 32 in PA OTCase. A tryptophan in position 146 (helix H5) in PF OTCase also structurally replaces an arginine at the same position in PA OTCase. Modeling studies already suggested that these residues would be part of a set of hydrophobic interactions between the trimeric subunits of the molecule and likely to play a role in its thermal stabilization (16). The structural results reported in this paper not only support this prediction but also present important features that could not be predicted from the model.

Within the monomer itself the comparison with PA OTCase does not reveal any specific characteristics related to thermal stabilization. As regards interactions between monomers within the trimeric subunits, an increase in ion pair networks with respect to PA OTCase was observed. This increase is very limited when compared with interactions stabilizing the trimeric organization in the mesophilic OTCase. One salt bridge also is observed at the interface between catalytic trimers in PF OTCase, involving K28 and E25. In PA OTCase, residues with similar charges are present at equivalent positions: R28 and D25. R28 is oriented toward the allosteric binding site and D25 is involved in stabilizing arginines 21 and 28 within the monomer. In the R state of the PA OTCase these residues cannot interact because of the difference of orientation between the trimers with respect to PF OTCase. It is not excluded, however, that they would interact in the T state, for which no three-dimensional structure is as yet available. These observations suggest a major role, regarding thermal stabilization, for the highly hydrophobic interactions observed between trimers. In PF OTCase these molecular contacts indeed replace the cluster of positive charges functioning as an allosteric effector binding site in PA OTCase.

What appears particularly remarkable in PF OTCase is the important role that the pattern of multimeric (dodecameric) association appears to play in enzyme stabilization, either within "catalytic trimers" or within "structural trimers." It seems as though the integrity of the whole dodecameric molecule at high temperature is based on the hydrophobic interactions occurring between catalytic trimers. A potential stabilizing role of increased subunit interactions via oligomerization was suggested long ago by Opitz *et al.* (32) on the basis of fragmentation studies on lactate dehydrogenase, or more recently by Kohlhoff *et al.* (33) from modeling studies of triosephosphate isomerase. The present crystallographic analysis of PF OTCase provides a concrete structural illustration of this idea, the outcome of which indeed indicates that oligomerization can play a major role in extreme thermal stabilization.

The comparison between PF and PA OTCases suggests that evolution apparently has designed two structures, which, through oligomerization, have achieved two very different biological properties—thermophily and allostery—starting from a trimer as a common catalytic motif. The large differ-

ences observed between the structures of the thermophilic and mesophilic OTCases thus reveal the great plasticity of the dodecamer, resulting in different conformations of 23-point group symmetry. A striking difference in quaternary structure appears to be the domain closure within the thermophilic monomer, an event that has been proposed to initiate the T-R allosteric transition in PA OTCase. Domain closure already is known to occur during the transition toward the active form of the paralogous enzyme aspartate carbamoyltransferase (21). This domain closure in PF OTCase indeed may have important effects because the binding sites for the two substrates are located between the two domains. The structure of PF OTCase therefore can be considered as functionally analogous to the R state of PA OTCase but in a quite different structural context.

One structural feature of PF OTCase is worth an additional comment. Several reports implicate a higher degree of compactness as a determinant of thermostability (27–29). The accessible area in PF OTCase is reduced relative to other trimeric OTCases. However, when compared with PA OTCase, the enzyme has a less compact quaternary structure, with larger channels and internal cavities. This appears as an unexpected feature for a thermophilic enzyme (34) and actually shows that higher compactness is not a prerequisite of thermophily, as generally believed.

The present analysis represents a step in the structural studies of the multienzymatic complexes used by thermophilic organisms to protect the thermosensitive and potentially toxic substrate carbamoylphosphate from the bulk of the aqueous phase through channeling between carbamoylphosphate synthetase and OTCase.

We thank Dr. Bart Devreese for the mass spectrometric analyses. This work was supported by the Fonds voor Wetenschappelijk Onderzoek-Vlaanderen (Contract 3G006896), by a Concerted Research Action between the Belgian State and the Vrije Universiteit Brussel, and by the Vlaams Actieprogramma voor Biotechnologie.

1. Woese, C. R., Kandler, O. & Wheelis, M. L. (1990) *Proc. Natl. Acad. Sci. USA* **87,** 4576–4578.
2. Stetter, K. O. (1996) *FEMS Microbiol. Rev.* **18,** 149–158.
3. Cunin, R., Glansdorff, N., Piérard, A. & Stalon, V. (1986) *Microbiol. Rev.* **50,** 314–352.
4. Davis, R. H. (1986) *Microbiol. Rev.* **50,** 280–313.
5. Glansdorff, N. (1996) in *Cellular and Molecular Biology*, ed. Neidhardt, F. (Am. Soc. Microbiol., Washington, DC), pp. 408–433.
6. Van de Casteele, M., Demarez, M., Legrain, C., Glansdorff, N. & Piérard, A. (1990) *J. Gen. Microbiol.* **136,** 1177–1183.
7. Sakanyan, V., Desmarez, L., Legrain, C., Charlier, D., Mett, I., Kochikyan, A. Savchenko, A., Boyen, A., Falmagne, P., Piérard, A. & Glansdorff, N. (1993) *Appl. Environ. Microbiol.* **59,** 3878–3888.
8. Legrain, C., Demarez, M., Glansdorff, N. & Piérard, A. (1995) *Microbiology* **141,** 1093–1099.
9. Van de Casteele, M., Legrain, C., Desmarez, L., Chen, P. G., Piérard, A. & Glansdorff, N. (1997) *Comp. Physiol. Biochem.*, **118A,** 463–473.
10. Tricot, C., Nguyen, V. T. & Stalon, V. (1993) *Eur. J. Biochem.* **215,** 833–839.
11. Tricot, C., Schmid, S., Baur, H., Villeret. V., Dideberg, O., Haas, D. & Stalon, V. (1994) *Eur. J. Biochem.* **221,** 555–561.
12. Nguyen, V. T., Baker, D. P., Tricot, C., Baur, H., Villeret, V., Dideberg O., Gigot, D., Stalon, V. & Haas, D. (1996) *Eur. J. Biochem.* **236,** 283–293.
13. Villeret, V., Tricot, C., Stalon, V. & Dideberg, O. (1995) *Proc. Natl. Acad. Sci. USA* **92,** 10762–10766.
14. Jin, L., Seaton, B. A. & Head, J. (1997) *Nat. Struct. Biol.* **4,** 622–625.
15. Marcq, S., Diaz-Ruano, A., Charlier, P., Dideberg, O., Tricot, C., Piérard, A. & Stalon, V. (1991) *J. Mol. Biol.* **220,** 9–12.
16. Legrain, C., Villeret, V., Roovers, M., Gigot, D., Dideberg, O., Piérard, A. & Glansdorff, N. (1997) *Eur. J. Biochem.* **247,** 1046–1055.
17. Roovers, M., Hethke, C., Legrain, C., Thomm, M. & Glansdorff, N. (1997) *Eur. J. Biochem.* **247,** 1038–1045.
18. Otwinowski, Z. (1993) in *Proceedings of the CCP4 Study Weekend: Data Collection and Processing, 29–30 January 1993*, eds. Sawyer, L., Isaacs, N. & Bailey, S. (Science and Engineering Research Council Daresbury Laboratory, Warrington, United Kingdom), pp 56–62.
19. Navaza, J. (1994) *Acta Crystallogr. A* **50,** 157–163.
20. Brünger, A. T. (1992) *A System for X-Ray Crystallography and NMR: X-PLOR Version 3.1* (Yale Univ. Press, New Haven, CT).
21. Lipscomb, W. N. (1994) *Adv. Enzymol. Relat. Areas Mol. Biol.* **68,** 67–151.
22. Argos, P., Rossmann, M. G., Grau, U. M., Zuber, H., Frank, G. & Tratschin, J. D. (1979) *Biochemistry* **18,** 5698–5703.
23. Kelly, C. A., Nishiyama, M., Ohnishi, Y., Beppu, T. & Birktoft, J. J. (1993) *Biochemistry* **32,** 3913–3922.
24. Korndörfer, I., Steipe, B., Huber, R., Tomschy, A. & Jaenicke, R. (1995) *J. Mol. Biol.* **246,** 511–521.
25. Yip, K. S. P., Stillman, T. J., Britton, K. K., Artymiuk, P. J., Baker, P. J., Sedelnikova, S. E, Engel, P. C., Pasquo, A., Chiaraluce, R., Consalvi, V., *et al.* (1995) *Structure* **3,** 1147–1158.
26. Day, M. W., Hsu, B. T., Joshua-Tor, L., Park, J. B., Zhou, Z. H., Adams, M. W. & Rees, D. C. (1992) *Protein Sci.* **1,** 1494–1507.
27. Russell, R. J., Ferguson, J. M., Hough, D. W., Danson, M. J. & Taylor, G. L. (1997) *Biochemistry* **36,** 9983–9994.
28. Chan., M. K., Mukund, S., Kletzin, A., Adams, M. W. & Rees, D. C. (1995) *Science* **267,** 1463–1469.
29. Goldman, A. (1995) *Structure (London)* **3,** 1277–1279.
30. Hennig, M., Darimont, B., Sterner, R., Kirschner, K. & Jansonius, J. N. (1995) *Structure (London)* **3,** 1295–1306.
31. Russell, R. J., Hough, D. W., Danson, M. J. & Taylor, G. L. (1994) *Structure (London)* **2,** 1157–1167.
32. Opitz, U., Rudolph, R., Jaenicke, R., Ericsson, L. & Neurath, H. (1987) *Biochemistry* **26,** 1399–1406.
33. Kohlhoff, M., Dahm, A. & Hensel, R (1996) *FEBS Lett.* **383,** 245–250.
34. Daniel, R. M., Dines, M. & Petach, H. (1996) *Biochem. J.* **317,** 1–11.
35. Nicholls, A., Sharp, K. A. & Honig, B. (1991) *Proteins* **11,** 281–296.
36. Kraulis, P. J. (1991) *J. Appl. Crystallogr.* **24,** 946–950.
37. Merritt, E. A. & Murphy, M. E. P. (1994) *Acta Crystallogr. D* **50,** 869–873.